AIAA JOURNAL
Vol. 31, No. 12, December 1993

Reliability and Nonlinear Supersonic Flutter of Uncertain Laminated Plates

D. G. Liaw* and Henry T. Y. Yang†
Purdue University, West Lafayette, Indiana 47907

It is the intent of this paper to study the geometrically nonlinear supersonic flutter characteristics of laminated composite thin-plate structures using a 48 degree-of-freedom rectangular plate element developed on the basis of the classical lamination theory. The aerodynamic pressure due to supersonic potential flow is simplified using the quasisteady first-order piston theory. Another intent is to study the reliability of laminated thin plates with structural uncertainties due to possible variabilities that occurred during the fabricating process. Interactive effects between the in-plane load and aerodynamic pressure for the uncertain plates are also studied. The stochastic finite element formulation is accomplished by including the effects of structural uncertainties. The stochastic solution procedure is based on the mean-centered second-moment perturbation technique. To evaluate the validity and to demonstrate the applicability of the present developments, a series of nonlinear free vibration and supersonic flutter analyses of isotropic and laminated composite thin plates are performed. The results quantify the effects of geometric nonlinearity on the mechanical behavior and structural reliability of the present laminated plates. Efforts are made to interpret the results so as to provide physical insight into the problems. Conversely, the present method and results may help to provide limits for the random variables to control the fabrication process.

Introduction

PANEL flutter in the supersonic flow falls in the category of self-excited oscillations. Small-amplitude linear structural theory indicates that there is a critical dynamic pressure value above which the panel motion becomes unstable and grows exponentially with time, whereas the inclusion of a geometrically nonlinear effect in the flutter analysis makes the panel motion generally restrained and bounded into a limit cycle oscillation.

Many investigators have studied the linear and nonlinear panel flutter behaviors. Analytical techniques such as the Galerkin method, direct integration method, harmonic balance method, and perturbation method have been used. A thorough and definitive survey of such studies was given by Dowell.[1,2] Another valuable monograph was written by Librescu.[3]

In addition to these analytical methods, finite element methods have been used by many investigators. Some brief reviews for such studies were given by, among others, Mei,[4] Han and Yang,[5] and Sarma and Varadan.[6] For the nonlinear supersonic flutter analysis of thin-plate structures, most studies were devoted to two-dimensional panels. Relatively fewer investigators treated the three-dimensional case, i.e., rectangular panels with finite aspect ratio. For example, Han and Yang[5] studied the nonlinear supersonic flutter behavior of simply supported and clamped square plates.

For the obvious advantages such as the high strength-to-weight ratio and high stiffness-to-weight ratio, etc., fiber-reinforced laminated composite materials have been increasingly used in the design and fabrication of thin-plate structures. For the laminated composite thin plates, although many aspects of their physical behaviors, such as buckling, linear and nonlinear vibrations, and linear flutter, have been widely studied, nonlinear flutter behaviors have been studied limitedly. It appears useful to formulate a laminated thin-plate finite element including geometric nonlinearity and aerodynamic pressure to study the nonlinear supersonic flutter behavior of laminated thin plates for practical applications.

Because of the difficulty frequently encountered in achieving quality control of manufacturing processes, structural variabilities that are random in nature may occur. These process-induced variabilities may include fiber size, volume fraction of fibers, fiber orientations, thickness of each lamina, and curvatures of the plate. Such variabilities will affect the achievable performance of strengths and stiffnesses of the finished plates and will also influence their structural reliabilities.

Many investigators studied the effects of such variabilities on the buckling, vibration, and flutter of thin-wall structures. Some recent brief reviews for such studies can be found in, among others, Refs. 7 and 8.

It is an objective of this study to investigate the effects of random structural uncertainties on the nonlinear supersonic flutter behavior and the reliability of uncertain laminated thin plates. The random structural uncertainties considered include modulus of elasticity, mass density, thickness, and fiber orientation of individual lamina, as well as initial geometric imperfections of the entire plate.

In the design of thin-plate structures, such as a panel in a wing, it is often necessary to consider the effect of in-plane stresses. Such an effect on the natural frequencies was studied previously by, among others, Mei and Yang.[9] Such an effect on the critical aerodynamic pressure or flutter speed was also studied previously by, among others, Bisplinghoff and Ashley,[10] Sander et al.,[11] and Han and Yang.[5] It is apparently of interest to study further the effect of in-plane stresses as a random variable on the critical aerodynamic pressure or flutter speed of the laminated thin plates with structural uncertainties.

In this study, the formulation of the 48-degree-of-freedom (DOF) rectangular laminated thin-plate element is based on that first derived from a 16-DOF rectangular plate element[12] and then a 48-DOF curved shell element.[13] The classical lamination theory is used. The effect of the transverse shear deformations is neglected. The aerodynamic pressure due to supersonic potential flow is described by the quasisteady first-order

Presented as Paper 91-1168 at the AIAA/ASME/ASCE/AHS/ASC 32nd Structures, Structural Dynamics, and Materials Conference, Baltimore, MD, April 8–10, 1991; received Jan. 15, 1993; revision received April 20, 1993; accepted for publication April 20, 1993.

*Graduate Research Assistant, School of Aeronautics and Astronautics; currently Senior Engineer, Sverdrup Technology, Inc., Brook Park, OH.

†Professor of Aeronautics and Astronautics and Dean of Schools of Engineering. Fellow AIAA.

piston theory.[10] The structural and aerodynamic dampings have a significant effect on the determination of the flutter characteristics. Such an effect has been studied previously by, among others, Librescu.[3] However, the effect of structural and aerodynamic dampings is not considered in this paper. In such a case, a quasistatic rather than a quasisteady aerodynamic supersonic theory is used.

The formulation includes the linear stiffness, initial stress, incremental stiffness, mass, and aerodynamic matrices. These matrices are random in nature, depending on the probabilistic properties of the uncertainties. A solution procedure within the framework of stochastic finite element method[14,15] is developed based on the mean-centered second-moment perturbation technique.

To evaluate the validity of the present finite element formulation and solution procedure, two examples were studied, for which alternative solutions are available for comparison. The first example is a nonlinear free vibration analysis of a laminated composite plate. The second example is a nonlinear supersonic flutter analysis of an isotropic square plate. To demonstrate the practical applicability of the present development, three more examples were studied: 1) nonlinear supersonic flutter analysis of a laminated composite plate, 2) reliability analysis of a laminated composite plate with structural uncertainties, and 3) reliability analysis of a laminated composite plate with structural uncertainties under random in-plane loads. Interactive effects between the in-plane load and aerodynamic pressure were also studied in the last example.

Based on the numerical results, the advantageous effects of considering geometrical nonlinearity on the supersonic flutter behavior and reliability analysis of the present uncertain laminated plates are discussed.

Formulation

An earlier finite element formulation developed by the authors for linear supersonic flutter and reliability analyses of laminated thin-plate and shell structures[7,8] is extended here to include the effect of geometrical nonlinearity. The rectangular element has 12 degrees of freedom at each of the four corner nodes: u, u_x, u_y, u_{xy}, v, v_x, v_y, v_{xy}, w, w_x, w_y, and w_{xy} where u, v, and w are the displacements in the x, y, and z directions, respectively. The linear stiffness formulation is derived based on bicubic Hermitian polynomial functions for the u, v, and w displacements, respectively, in the same fashion as those derived in Refs. 12 and 13.

Equations of Motion

The equations of motion for a thin elastic plate element may be derived using Hamilton's principle. The equations of motion for the element can be obtained as

$$[m]\{\ddot{q}\} + ([k] + N[\sigma] + \tfrac{1}{2}[n_1] + \tfrac{1}{3}[n_2] + \lambda[a])\{q\} = \{0\} \tag{1}$$

where N is the initial in-plane stress, and $[m]$, $[k]$, $[\sigma]$, $[n_1]$, $[n_2]$, and $[a]$ are the consistent mass, linear stiffness, initial stress, first-order incremental stiffness, second-order incremental stiffness, and aerodynamic matrices, respectively. The aerodynamic pressure parameter λ is defined as

$$\lambda = \frac{2q}{\sqrt{M_\infty^2 - 1}} \tag{2}$$

where q is the aerodynamic pressure and M_∞ is the Mach number. Equation (1) can be written in the incremental form as

$$[m]\{\Delta\ddot{q}\} + ([k] + N[\sigma] + [n_1] + [n_2] + \lambda[a])\{\Delta q\} = \{0\} \tag{3}$$

The previous equation can also be written as

$$[m]\{\Delta\ddot{q}\} + ([k_T] + \lambda[a])\{\Delta q\} = \{0\} \tag{4}$$

The matrix $[k_T]$ is called the tangential stiffness matrix and is written as

$$[k_T] = \iint_A [B_L + B_{NL}(q)]^T \begin{bmatrix} A & B \\ B & D \end{bmatrix} [B_L + B_{NL}(q)]\mathrm{d}A + \iint_A [G]^T[H][G]\mathrm{d}A \tag{5}$$

The matrices $[B_L]$ and $[B_{NL}(q)]$ relate the incremental strains $\{\mathrm{d}\epsilon\}$ to the incremental displacements $\{\Delta q\}$ as

$$\{\mathrm{d}\epsilon\} = [B_L + B_{NL}(q)]\{\Delta q\} \tag{6}$$

where $[B_L]$ is the same as that for the linear case. The strain-displacement matrix due to geometrically nonlinear effect is $[B_{NL}]$. Matrices $[G]$ and $[H]$ were given by Kapania and Yang.[16] The consistent mass matrix can be obtained by following a general procedure outlined in common text.[17]

The aerodynamic matrix can be derived by following the procedure proposed by, among others, Sander et al.[11] and Han and Yang.[5] In this study, the aerodynamic matrix is formulated based on the two-dimensional quasisteady supersonic flow theory. The Mach number is limited to be approximately beyond 1.6.

The random field of a single structural uncertainty is described as a random amplitude multiplied by a deterministic spatial function. The detailed formulation can be found in Refs. 7 and 8.

By assembling the finite elements for the entire plate system and applying the kinematic boundary conditions, the equations of motion for the entire system can be expressed in the same form as Eq. (4) by capitalizing all of the symbols:

$$[M]\{\Delta\ddot{Q}\} + ([K_T] + \lambda[A])\{\Delta Q\} = \{0\} \tag{7}$$

Solution Procedures

To solve Eq. (7), the displacement vector is assumed as an exponential function of time

$$\{\Delta Q\} = \{\Delta\bar{Q}\}e^{\alpha t} \tag{8}$$

where α is a complex number. By substituting Eq. (8) into Eq. (7), the equations of motion become

$$(k[M] + [K_T] + \lambda[A])\{\Delta\bar{Q}\} = \{0\} \tag{9}$$

where $k = \alpha^2$.

To solve the nonlinear eigenvalue Eq. (9), an iterative procedure is used.[4,5,18] For a given set of aerodynamic pressure λ, in-plane force N, mode number, and maximum amplitude, the iteration starts from a corresponding initial mode shape obtained from linear flutter analysis, with amplitude scaled up by a small factor. Based on this initial mode shape, the tangential stiffness matrix $[K_T]$ is formed, and an eigenvalue and its corresponding eigenvector are found. This eigenvector is then scaled up again, and the iteration continues until the convergence criterion $|\psi|$ for k is achieved:

$$|\psi| = \left|\frac{\Delta k_i}{k_i}\right| \leq 10^{-3} \tag{10}$$

where Δk_i is the change in eigenvalue during the ith iterative cycle.

As indicated by previous investigators,[4-6] when $\lambda = 0$, the problem is reduced to that of finding the in-vacuo frequencies for the nonlinear free vibration of plates. As dynamic pressure λ is increased from zero, two of these eigenvalues will usually approach each other and coalesce to k_{cr} at $\lambda = \lambda_{\mathrm{cr}}$ and become a complex conjugate pair for $\lambda > \lambda_{\mathrm{cr}}$. Here λ_{cr} is considered to be that value of λ at which the first coalescence occurs for a specific amplitude of the limit cycle oscillation.

Results

To evaluate the present finite element formulation and solution procedure and to study the effects of various uncertain parameters on the reliability and nonlinear supersonic flutter behavior of laminated plates, a series of nonlinear free vibration and nonlinear supersonic flutter analyses of thin plates were performed with results presented, discussed, and physically interpreted. Interactive effects between the in-plane force and critical aerodynamic pressure were also studied with the effects of various uncertain parameters included.

In all of the examples, a sufficiently fine Gaussian grid (5 × 5) was used for numerical integration to obtain the element linear stiffness, initial stress, incremental stiffness, mass, and aerodynamic matrices. This grid was shown numerically to be sufficiently fine and accurate for all of the present examples. On the other hand, a convergence study of the finite element meshes was conducted for each of the following examples. The mesh chosen for each example was among the ones that yielded converged results as the mesh was successively refined. All calculations were carried out using a CYBER 205 vectorized supercomputer at Purdue University.

Nonlinear Free Vibration of a Simply Supported Laminated Composite Square Plate

The example square plate studied was assumed as simply supported with $u_x = u_{xy} = v = v_y = w = w_y = 0$ at $x = \pm L/2$ and $u = u_x = v_y = v_{xy} = w = w_x = 0$ at $y = \pm L/2$. The length L of the plate was assumed as 10 in. The laminate construction was assumed as $[0_{10}/90_{10}]$ with thickness of each lamina equal to 0.005 in. It is an antisymmetric cross-ply laminate. The in-plane and bending stiffnesses in the x and y directions are the same. The material of each lamina was assumed as a graphite/epoxy with the following properties: $E_L = 30 \times 10^6$ psi, $E_T = 0.75 \times 10^6$ psi, $G_{LT} = 0.375 \times 10^6$ psi, $\nu_{LT} = 0.25$, $\rho = 0.145 \times 10^{-3}$ lb-s²/in.⁴.

Two 2 × 2 finite element meshes with appropriate boundary conditions were used to model a quarter of the plate in analyzing the nonlinear periods of the first and second modes, respectively. For the first mode, the symmetric boundary conditions along $x = 0$ and $y = 0$ were assumed as $u = u_y = v_x = v_{xy} = w_x = w_{xy} = 0$ and $u_y = u_{xy} = v = v_x = w_y = w_{xy} = 0$, respectively. For the second mode, the symmetric boundary condition along $x = 0$ and the antisymmetric boundary condition along $y = 0$ were assumed as $u = u_y = v_x = v_{xy} = w_x = w_{xy} = 0$ and $u = u_x = v_y = v_{xy} = w = w_x = 0$, respectively. The range for the amplitude ratio w_{max}/h for both modes was taken between 0 and 2. Figure 1 shows the results for the period ratio of the first two modes (T_{NL}/T_L) of the plate. The

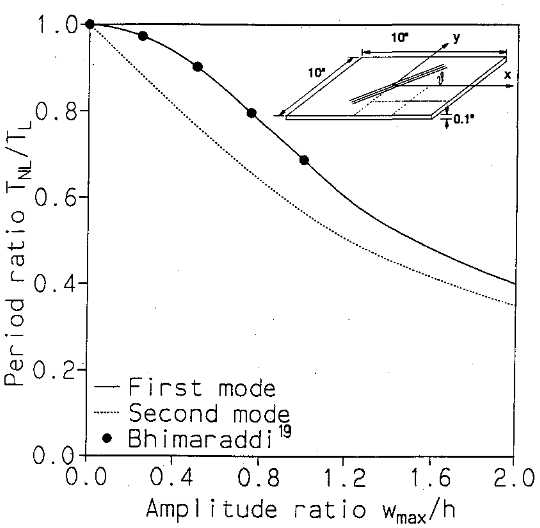

Fig. 1 Period ratios (T_{NL}/T_L) for the first two modes of a simply supported laminated $[0_{10}/90_{10}]$ square plate with various amplitude ratios (w_{max}/h).

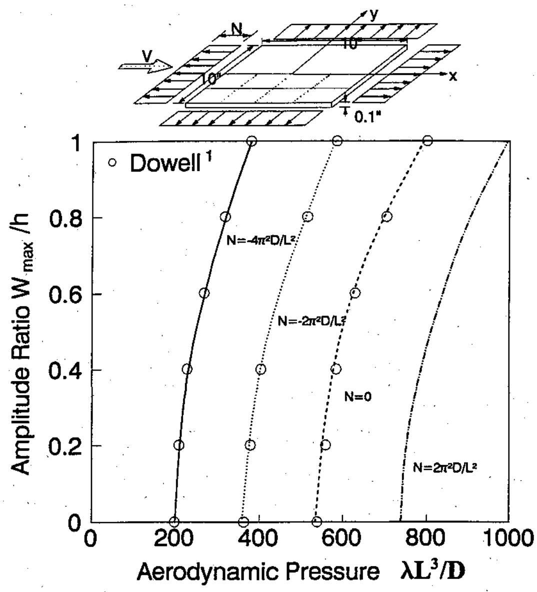

Fig. 2 Limit cycle amplitude vs aerodynamic pressure plots for a simply supported isotropic square plate under various biaxial in-plane loads N.

period ratio for the fundamental mode was obtained previous by Bhimaraddi[19] using the one-term Galerkin method. His results are also plotted for comparison. Excellent agreement is seen. It is seen that the geometric nonlinearity has a similarly pronounced effect on reducing the period of the second mode as for the first mode.

Nonlinear Supersonic Flutter of a Simply Supported Isotropic Square Plate

The example square plate studied was assumed as simply supported with $u_x = u_{xy} = v = v_y = w = w_y = 0$ at $x = \pm L/2$ and $u = u_x = v_y = v_{xy} = w = w_x = 0$ at $y = \pm L/2$. The length L and the thickness h of the plate were assumed as 10 and 0.1 in., respectively. The material properties were assumed to be those for 6061-T6 aluminum: $E = 10 \times 10^6$ psi, $\nu = 0.3$, and $\rho = 0.254 \times 10^{-3}$ lb-s²/in.⁴.

A 4 × 2 finite element mesh was used to model a half of the plate. The boundary conditions along $y = 0$ were assumed as $u_y = u_{xy} = v = v_x = w_y = w_{xy} = 0$. Figure 2 shows the results for the amplitude of the limit cycle oscillation of the square plate vs the various aerodynamic pressures. Four values of initial biaxial in-plane forces—$N = 2\pi^2 D/L^2$, 0, $-2\pi^2 D/L^2$, and $-4\pi^2 D/L^2$—were considered where D is the flexural rigidity of the plate with $D = Eh^3/12(1 - \nu^2)$. The problem was studied previously by Dowell[1] using a time integration method based on six modes. His results are also plotted for comparison. The agreement is good. It is seen, as expected, that the in-plane compression has an effect of reducing the critical aerodynamic pressure in both linear and nonlinear flutter analyses. It is also seen that the geometric nonlinearity has an advantageous effect in increasing the critical aerodynamic pressure.

Nonlinear Supersonic Flutter of a Simply Supported Laminated Composite Square Plate

The example square plate studied was assumed as simply supported with $u_x = u_{xy} = v = v_y = w = w_y = 0$ at $x = \pm L/2$ and $u = u_x = v_y = v_{xy} = w = w_x = 0$ at $y = \pm L/2$. The length L of the plate was assumed as 10 in. The laminate construction was assumed as $[90/\pm 45/0]_s$ with the thickness of each lamina equal to 0.005 in. The material of each lamina was assumed to be graphite/epoxy with the following properties: $E_L = 20 \times 10^6$ psi, $E_T = 1.5 \times 10^6$ psi, $G_{LT} = 0.75 \times 10^6$ psi, $\nu_{LT} = 0.25$, and $\rho = 0.145 \times 10^{-3}$ lb-s²/in.⁴.

A 4 × 2 finite element mesh was used to model a half of the plate. The boundary conditions along $y = 0$ were assumed to

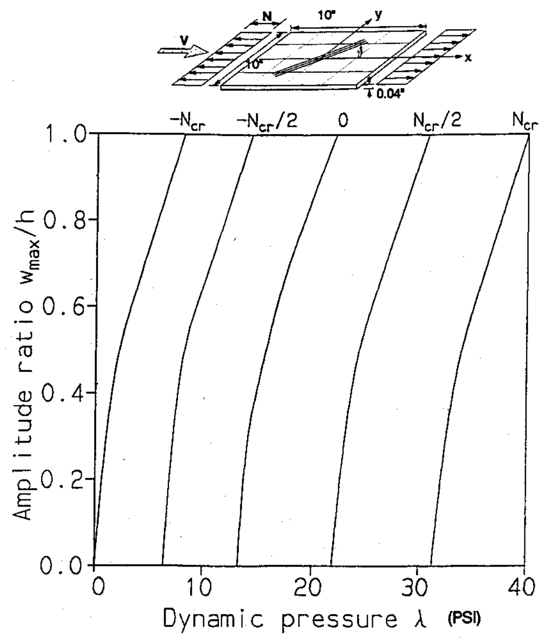

Fig. 3 Plots for limit cycle amplitude vs dynamic pressure for a simply supported graphite/epoxy laminated $[90/\pm 45/0]_s$ square plate under various uniaxial in-plane loads.

be $u_y = u_{xy} = v = v_x = w_y = w_{xy} = 0$. Figure 3 shows the results for the amplitude of the limit cycle oscillation of the laminated square plate vs various aerodynamic pressures. Five values of initial uniaxial in-plane forces were considered. These were N_{cr}, $N_{cr}/2$, 0, $-N_{cr}/2$, and $-N_{cr}$ where N_{cr} is the critical uniaxial buckling load for the plate. It is seen that the in-plane compression has an effect of reducing the critical aerodynamic pressure in both linear and nonlinear ranges. On the other hand, the in-plane tension has an effect of increasing the critical aerodynamic pressure. As expected, the geometric nonlinearity has an advantageous effect of increasing the critical aerodynamic pressure for all five cases.

Reliability of a Simply Supported Laminated Square Plate with Structural Uncertainties

The reliability of an eight-ply $[\theta_1/\theta_2/\theta_3/\theta_4]_s$ graphite/epoxy laminated square plate with structural uncertainties was investigated. The geometric and boundary conditions of the square plate and the material properties of each lamina were assumed to be the same as those of the previous example.

The orientation of the fibers in each lamina was considered as a random variable. Practically speaking, not all of the fibers in the same lamina are oriented with exactly the same angle. On the other hand, it would be computationally formidable to treat each of the fibers in the same lamina as a random variable. Thus the single random variable model assumed in this study implies that all of the fibers have the same orientation in the same lamina and are random in the same fashion. Such a model neglects the mutually compensating effects due to the uncertainties of each individual fiber, which is certainly more conservative and yields relatively lower reliability. The mean values of the fiber orientation $\theta_i (i = 1,\ldots, 4)$ were assumed as 90, 45, -45, and 0 deg, respectively. The standard deviation of the fiber orientation of each lamina was assumed to be $\sigma(\theta) = 5$ deg.

The variability of the volume fraction of fibers was accounted for using the modulus of elasticity as a random variable. The other structural uncertainties include the thickness of each lamina and the initial geometric imperfections over the entire plate. The coefficients of variation (COV) for the modulus of elasticity and thickness of each lamina were assumed to be COV(E) = 5% and COV(h) = 5%, respectively. The shape of the initial geometric imperfection was assumed to be the same as the critical buckling mode as

$$w_i(x, y) = \delta h \cos \frac{\pi x}{L} \cos \frac{\pi y}{L} \tag{11}$$

where the x and y coordinates are parallel with the horizontal and vertical edges of the square plate, respectively, and the origin of the coordinates coincides with the center of the plate; random variable δ was assumed to be of Gaussian distribution with zero mean and standard deviation of 0.05.

The standard deviations and coefficients of variation of the critical aerodynamic pressure due to the aforementioned uncertainties in each lamina of the plate were obtained using the present stochastic finite element method. Thus the standard deviations and coefficients of variation of the critical aerodynamic pressure due to the correlated effect of uncertain

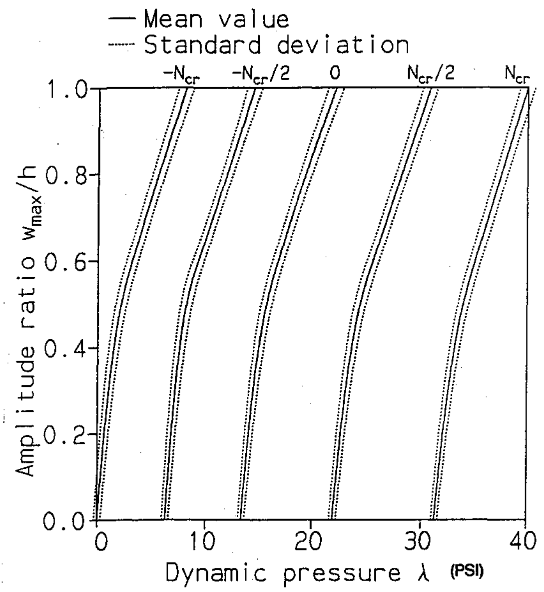

Fig. 4 Mean values and standard variations of critical aerodynamic pressure for the simply supported graphite/epoxy laminated $[90/\pm 45/0]_s$ square plate with uncertain fiber orientations under various uniaxial in-plane loads (zero correlated among all layers).

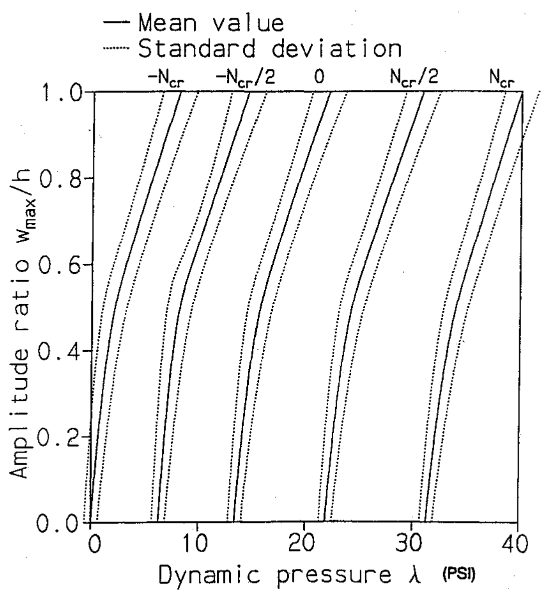

Fig. 5 Mean values and standard variations of critical aerodynamic pressure for the simply supported graphite/epoxy laminated $[90/\pm 45/0]_s$ square plate with uncertain fiber orientations under various uniaxial in-plane loads (fully correlated among all layers).

parameters among all eight laminae can be obtained. Two extreme conditions, zero and full correlations among all eight laminae, were considered. For the fully correlated condition, a single random variable was used to represent the uncertainties in all laminae. It implied that the uncertainty through the thickness was uniform. On the other hand, for the zero correlated condition, an individual random variable was used to represent the uncertainty in each lamina. The nonuniformity of the uncertainty through the thickness was considered. In that case, the effect of uncertainty on each lamina tended to compensate for each other in a random fashion. Figures 4 and 5 show the mean values and standard deviations of the critical aerodynamic pressure of the laminated plate with uncertain fiber orientations under various in-plane forces for zero and fully correlated conditions, respectively. The effect of nonlinearity becomes apparent; the standard deviations are increased when amplitude ratios are increased for all of the five in-plane loading conditions and for both correlated conditions.

Based on the mean value and the standard deviation (or coefficient of variation) of the critical aerodynamic pressure, the probability distribution curve was obtained for the uncertain parameter. The reliability for a specified aerodynamic pressure could be obtained by integrating the portion of the area on the right-hand side of the specified aerodynamic pressure and under the probability distribution curve as shown in Fig. 6. It is noted that the reliability is 0.5 when the specified aerodynamic pressure is equal to the mean value of the critical aerodynamic pressure, i.e., the probability of the critical aerodynamic pressure is 50% above and 50% below the specified aerodynamic pressure.

Figures 6–8 show the reliability boundaries for supersonic aerodynamic flutter for the plate with fiber orientations, modulus of elasticity, and thickness, respectively, as uncertain parameters. The flow is assumed in the same direction as the zero degree fiber ($\theta = 0$ deg). It is seen that the reliability boundaries are lowest as each random parameter occurred in the second and seventh laminae where the fiber angle $\theta = 45$ deg. Obviously, the reliability is not only dominated by the distance of the lamina from the neutral surface along the thickness direction but also by the fiber orientation of the lamina relative to the flow direction. For example (see Fig. 6), the reliability curve for layers 3 and 6 (with $\theta = -45$ deg) is lower than that for the outmost layers 1 and 8 (with $\theta = 90$ deg). The effect on the reduction of reliability due to the randomness of the fiber orientation for the layers with $\theta = -45$ deg is obviously more dominant than that for the layers with $\theta = 90$ deg. The reliability curve for layers 2 and 7 is obviously lower than that for layers 3 and 6 because layers 2 and 7 are further from the neutral plane and thus carry more bending stresses, whereas all of the four layers have the same fiber angle of 45 deg. It is also seen that the zero correlated case results in higher reliabilities than the fully correlated case due to the compensation effect among the laminas in a random fashion.

Figures 9–11 show the reliability boundaries of the plate with random geometric imperfections, uncertain mass density, and uniformly distributed random in-plane loads, respectively. Two values of coefficients of variation for the uncertain amplitude of the geometric imperfection, $COV(\delta) = 0.05$ and 0.1, were considered. The value of the coefficient of variation for the uncertain mass density was assumed to be $COV(\rho) = 0.05$. Two values of standard deviations for the uncertain in-plane load, $\sigma(N/N_{cr}) = 0.05$ and 0.1, were considered. It is seen that these three uncertain parameters have the

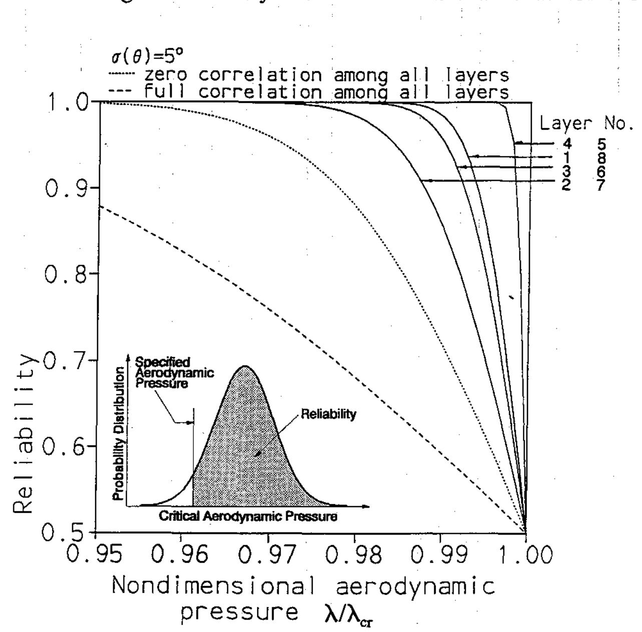

Fig. 6 Reliability of the simply supported graphite/epoxy laminated $[90/\pm45/0]_s$ square plate in supersonic flow with uncertain fiber orientations ($N = N_{cr}$, $w_{max}/h = 1.0$, $\sigma(\theta) = 5$ deg).

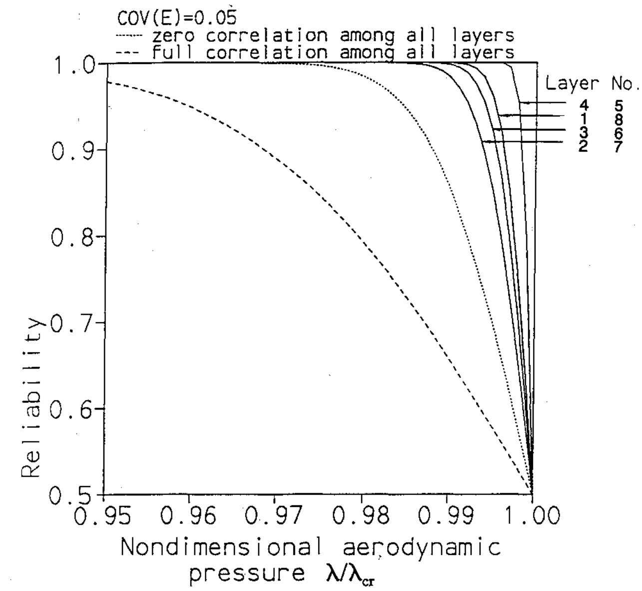

Fig. 7 Reliability of the simply supported graphite/epoxy laminated $[90/\pm45/0]_s$ square plate in supersonic flow with uncertain moduli of elasticity ($N = N_{cr}$, $w_{max}/h = 1.0$, $COV(E) = 0.05$).

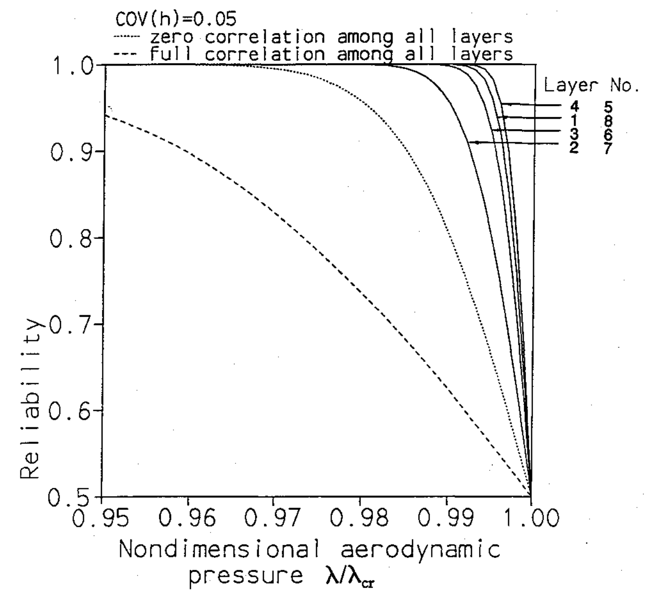

Fig. 8 Reliability of the simply supported graphite/epoxy laminated $[90/\pm45/0]_s$ square plate in supersonic flow with uncertain thickness ($N = N_{cr}$, $w_{max}/h = 1.0$, $COV(h) = 0.05$).

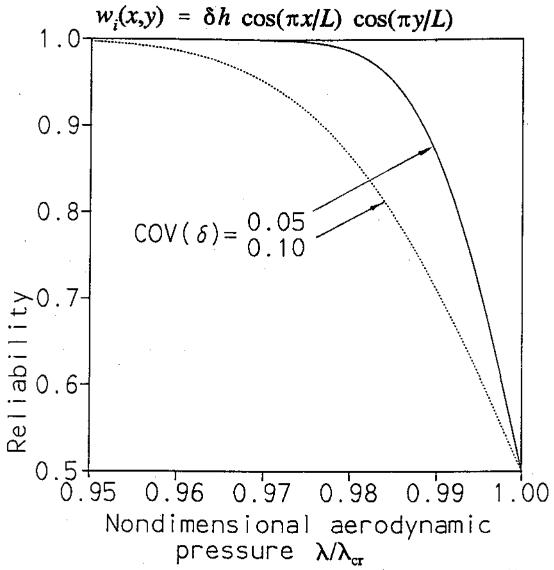

Fig. 9 Reliability of the simply supported graphite/epoxy laminated $[90/\pm45/0]_s$ square plate in supersonic flow with uncertain amplitude of geometric imperfections ($N = N_{cr}$, $w_{max}/h = 1.0$).

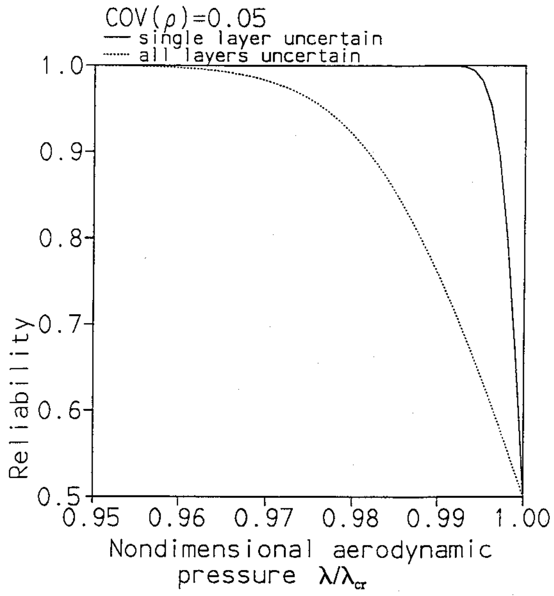

Fig. 10 Reliability of the simply supported graphite/epoxy laminated $[90/\pm45/0]_s$ square plate in supersonic flow with uncertain mass density ($N = N_{cr}$, $w_{max}/h = 1.0$, COV(ρ) = 0.05).

obvious effects on reducing the structural reliability against supersonic flutter. These effects are quantified in the figures for the parameter values assumed.

In practical application, it is possible that all of the previous uncertain parameters occur simultaneously in a certain random fashion. Figure 12 shows the combined effects of all of these uncertain parameters on the structural reliability boundaries for the subject plate in supersonic flow. Two sets of coefficients of variation (or standard deviations) of the six structural uncertain parameters were assumed, as listed in Fig. 12, to cover ranges of practical significance. Each uncertain parameter was assumed to be zero or fully correlated among all of the eight layers. It is seen that the two reliability curves for the fully correlated case are significantly lower than the two for the zero correlated case, respectively. Obviously, the random compensation effects among the six uncertain parameters with zero correlation tend to increase the reliability. The fully correlated curve for case 2 as shown in Fig. 12 definitely yields much lower reliability than any individual curve with only one uncertain parameter as shown in Figs. 6–11.

Nonlinear Supersonic Flutter of a Simply Supported Laminated Square Plate with Structural Uncertainties Under Uniform and Linearly Varying, Nonzero-Mean, Random In-Plane Loads

To study the interactive effects between the in-plane load and aerodynamic pressure, the same plate was further studied by including the random effect of nonzero-mean in-plane loads. The mean values of the in-plane loads were varied from $-N_{cr}$ to N_{cr}. Two sets of coefficients of variation (or standard deviations) for all of the six uncertain parameters were assumed, as listed in Fig. 13. Both zero and full correlative conditions among all of the uncertain parameters were considered.

Figures 13 and 14 show the mean values and the standard deviations of the critical aerodynamic pressure in the form of interactive stability boundaries, for the plates with amplitude ratio of 1.0 and 2.0, respectively, under uniformly distributed

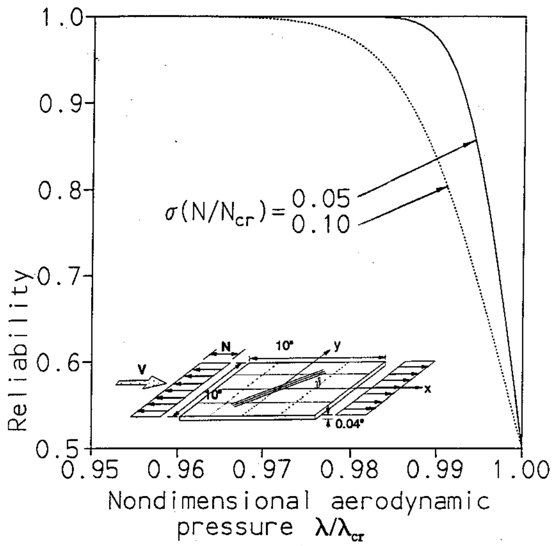

Fig. 11 Reliability of the simply supported graphite/epoxy laminated $[90/\pm45/0]_s$ square plate in supersonic flow with uncertain in-plane compressive loads ($N = N_{cr}$, $w_{max}/h = 1.0$).

case	COV(E)	COV(h)	σ(θ)	COV(ρ)	COV(δ)	σ(N/N$_{cr}$)
1	0.02	0.02	2°	0.02	0.02	0.02
2	0.05	0.05	5°	0.05	0.05	0.05

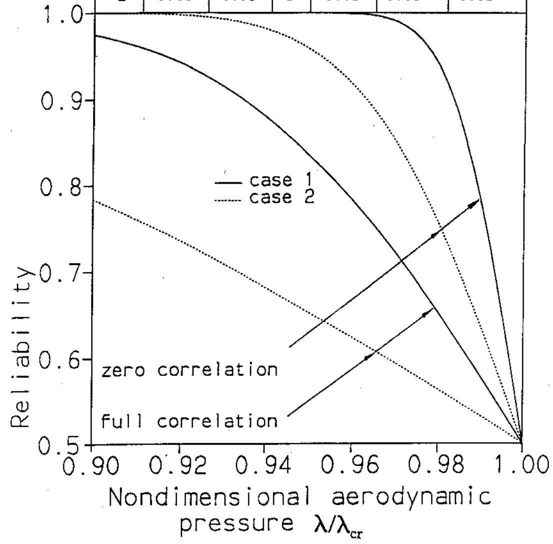

Fig. 12 Reliability of the simply supported graphite/epoxy laminated $[90/\pm45/0]_s$ square plate in supersonic flow with six uncertain parameters ($N = N_{cr}$, $w_{max}/h = 1.0$).

in-plane loads. The effects of these random parameters with currently assumed values on the reduction of these stability boundaries were quantified. It is apparent that, for case 2 with full correlation condition, the boundary is significantly reduced. It is of interest to note that the relationship between the critical aerodynamic pressure and the uniformly distributed in-plane load is not too far from being linear for all cases in both figures.

The general trends of the curves in Figs. 13 and 14 appear to be similar. Although the standard deviations for the critical aerodynamic pressure are larger in the case of amplitude ratio $w_{max}/h = 2.0$ (Fig. 14) than those in the case of $w_{max}/h = 1.0$ (Fig. 13), the differences of coefficient of variation, defined as standard deviation divided by mean values, between the two

case	COV(E)	COV(h)	σ(θ)	COV(ρ)	COV(δ)	σ(N/N$_{cr}$)
1	0.02	0.02	2°	0.02	0.02	0.02
2	0.05	0.05	5°	0.05	0.05	0.05

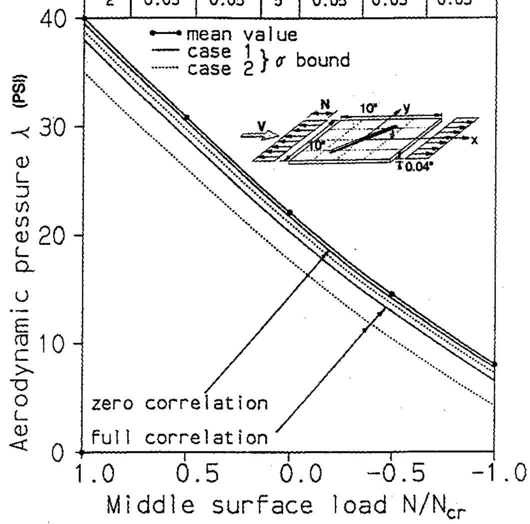

Fig. 13 Interactive effects between uniformly distributed in-plane load and aerodynamic pressure for the simply supported graphite/epoxy laminated $[90/\pm45/0]_s$ square plate with six uncertain parameters ($w_{max}/h = 1.0$).

case	COV(E)	COV(h)	σ(θ)	COV(ρ)	COV(δ)	σ(N/N$_{cr}$)
1	0.02	0.02	2°	0.02	0.02	0.02
2	0.05	0.05	5°	0.05	0.05	0.05

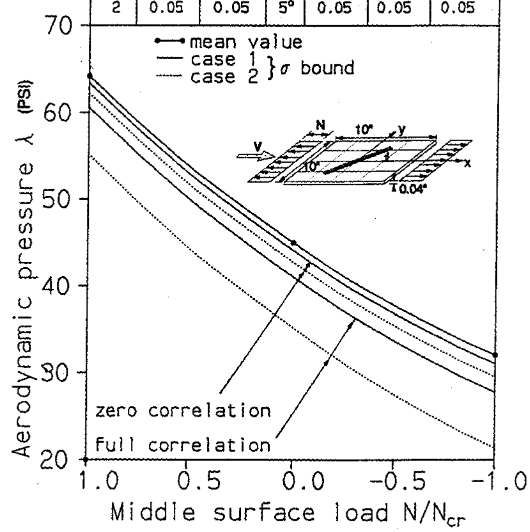

Fig. 14 Interactive effects between uniformly distributed in-plane load and aerodynamic pressure for the simply supported graphite/epoxy laminated $[90/\pm45/0]_s$ square plate with six uncertain parameters ($w_{max}/h = 2.0$).

case	COV(E)	COV(h)	σ(θ)	COV(ρ)	COV(δ)	σ(N/N$_{cr}$)
1	0.02	0.02	2°	0.02	0.02	0.02
2	0.05	0.05	5°	0.05	0.05	0.05

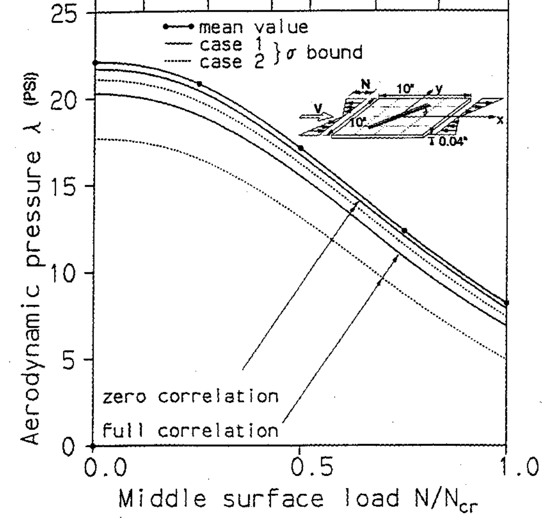

Fig. 15 Interactive effects between linearly distributed in-plane load and aerodynamic pressure for the simply supported graphite/epoxy laminated $[90/\pm45/0]_s$ square plate with six uncertain parameters ($w_{max}/h = 1.0$).

case	COV(E)	COV(h)	σ(θ)	COV(ρ)	COV(δ)	σ(N/N$_{cr}$)
1	0.02	0.02	2°	0.02	0.02	0.02
2	0.05	0.05	5°	0.05	0.05	0.05

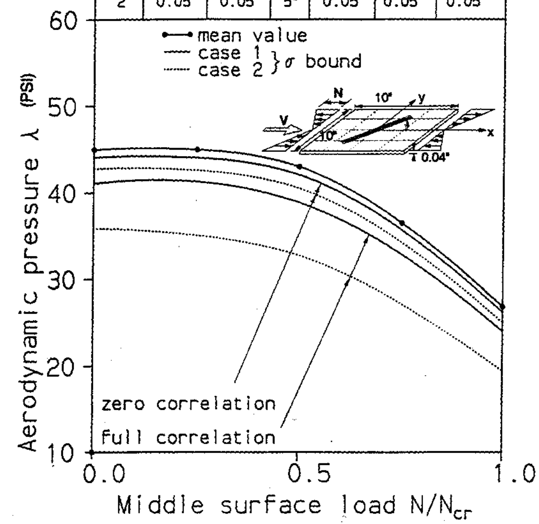

Fig. 16 Interactive effects between linearly distributed in-plane load and aerodynamic pressure for the simply supported graphite/epoxy laminated $[90/\pm45/0]_s$ square plate with six uncertain parameters ($w_{max}/h = 2.0$).

cases are small. It is seen in both figures that, as the in-plane compression increases, the mean value of the critical aerodynamic pressure decreases, but the coefficient of variation of the critical aerodynamic pressure increases. For example (see case 2 with fully correlated condition in Fig. 13), the mean value and the coefficient of variation of the critical aerodynamic pressure of the plate under in-plane load $N/N_{cr} = 0.5$ are 30.8 psi and 0.16 (=4.8/30.8), respectively. The mean value decreases and the coefficient of variation increases to 14.8 psi and 0.27 (=4.0/14.8), respectively, when the in-plane load is -0.5. Such phenomenon implies that as the in-plane compression is larger, the uncertain parameters have a more pronounced effect on the critical aerodynamic pressure.

A problem of practical significance is the flutter of a rectangular panel of a wing subjected to bending moments due to both lift and drag forces. As a result, the in-plane stresses are not uniformly distributed. It is of interest to study a panel with linearly varying in-plane stresses. Figures 15 and 16 show the mean values and the standard deviations of the critical aerodynamic pressure for the plates with amplitude ratio of 1.0 and 2.0, respectively, under linearly distributed in-plane loads. Again, the effects of the currently assumed random parameters on the reduction of these stability boundaries were quantified. It is interesting to see that the relationship between the critical aerodynamic pressure and the linearly distributed in-plane load is now far from being linear.

It is also seen in both figures that as the magnitude of the linearly distributed in-plane load increases, the mean value of the critical aerodynamic pressure decreases, but the coefficient of variation of the critical aerodynamic pressure increases. This phenomenon was also observed in Figs. 13 and 14.

Concluding Remarks

A 48-DOF rectangular stochastic laminated thin-plate finite element with probabilistic material properties, uncertain geometry, and random in-plane loads has been formulated. The solution procedure was based on the mean-centered second-moment perturbation technique.

The current results have been compared with alternative solutions in the deterministic cases of nonlinear vibration and nonlinear supersonic flutter analyses. The effects of these uncertain parameters on the nonlinear supersonic flutter and reliability have been studied. The interactive effects between the in-plane load and aerodynamic pressure were also studied and quantified for the present sets of assumed random parameters. Such interactive stability boundaries were shown close to being linear when the in-plane load was uniformly distributed and far from being linear when the in-plane load was linearly distributed. It is also seen that as the magnitude of the uniformly distributed in-plane compression or the linearly distributed in-plane load becomes larger, the uncertain parameters have a more pronounced effect on the scattering of the critical aerodynamic pressure.

In this study, ranges of values for each random parameter were assumed, and the results obtained quantify the effects of these parameters on the reliabilities of the present laminated plates subjected to in-plane force and supersonic aerodynamic pressure. However, it is hard to evaluate the relative importance of these random uncertainties since these effects are dependent on the specific values assumed. One must quantify the practical ranges of values of these random variables as based on the actual fabrication process. Conversely, based on the method and results presented here, one could also give limits of these random variables to control the fabrication process.

These quantified data may also provide structural designers with some physical insight into the effects of possible uncertain parameters. Such physical insight and the quantified data may be helpful in the design of more reliable laminated composite plate structures.

The present formulation and solution procedure are general and simple so that extensions can be made to include some more interesting effects, such as transverse shear deformations for thicker plates, aerodynamic nonlinearity, and structural and aerodynamic dampings.

Acknowledgments

This study was sponsored by the National Science Foundation through Grant ECE-8516915. Technical guidance from S. C. Liu is acknowledged.

References

[1]Dowell, E. H., "Nonlinear Oscillations of a Fluttering Plate," *AIAA Journal*, Vol. 4, No. 7, 1966, pp. 1267–1275.

[2]Dowell, E. H., "Nonlinear Oscillations of a Fluttering Plate II," *AIAA Journal*, Vol. 5, No. 10, 1967, pp. 1856–1862.

[3]Librescu, L., *Elastostatics and Kinetics of Anisotropic and Heterogeneous Shell-Type Structures*, Noordhoff International, Leyden, The Netherlands, 1975.

[4]Mei, C., "A Finite-Element Approach for Nonlinear Panel Flutter," *AIAA Journal*, Vol. 15, No. 8, 1977, pp. 1107–1110.

[5]Han, A. D., and Yang, T. Y., "Nonlinear Panel Flutter Using High-Order Triangular Finite Elements," *AIAA Journal*, Vol. 21, No. 10, 1983, pp. 1453–1461.

[6]Sarma, B. S., and Varadan, T. K., "Nonlinear Panel Flutter by Finite-Element Method," *AIAA Journal*, Vol. 26, No. 5, 1988, pp. 566–574.

[7]Liaw, D. G., and Yang, H. T. Y., "Reliability of Initial Compressed Uncertain Laminated Plates in Supersonic Flow," *AIAA Journal*, Vol. 29, No. 6, 1991, pp. 952–960.

[8]Liaw, D. G., and Yang, H. T. Y., "Reliability of Uncertain Laminated Shells Due to Buckling and Supersonic Flutter," *AIAA Journal*, Vol. 29, No. 10, 1991, pp. 1698–1708.

[9]Mei, C., and Yang, T. Y., "Free Vibrations of Finite Element Plates Subjected to Complex Middle-Plane Force Systems," *Journal of Sound and Vibration*, Vol. 23, No. 2, 1972, pp. 145–156.

[10]Bisplinghoff, R. L., and Ashley, H., *Principles of Aeroelasticity*, Wiley, New York, 1962.

[11]Sander, G., Bon, C., and Geradin, M., "Finite Element Analysis of Supersonic Panel Flutter," *International Journal for Numerical Methods in Engineering*, Vol. 7, No. 3, 1973, pp. 379–394.

[12]Bogner, F. K., Fox, R. L., and Schmit, L. A., "The Generation of Interelement-Compatible Stiffness and Mass Matrices by the Use of Interpolation Formulas," *Proceedings of the Conference on Matrix Methods in Structural Mechanics*, Air Force Flight Dynamics Lab., TR-66-80, Dayton, OH, Nov. 1966, pp. 397–444.

[13]Yang, T. Y., "High Order Rectangular Shallow Shell Finite Element," *Journal of Engineering Mechanics Division, ASCE*, Vol. 99, No. EM1, 1973, pp. 157–181.

[14]Vanmarcke, E., Shinozuka, M., Nakagiri, S., Schueller, G. I., and Grigoriu, M., "Random Fields and Stochastic Finite Elements," *Structural Safety*, Vol. 3, Nos. 3, 4, 1986, pp. 143–166.

[15]Nakagiri, S., and Hisada, T., *An Introduction to Stochastic Finite Elements*, Baifukan, Tokyo, 1987 (in Japanese).

[16]Kapania, R. K., and Yang, T. Y., "Formulation of an Imperfect Quadrilateral Doubly Curved Shell Element for Postbuckling Analysis," *AIAA Journal*, Vol. 24, No. 2, 1986, pp. 310, 311.

[17]Zienkiewicz, O. C., *The Finite Element Method*, 3rd ed., McGraw-Hill, London, 1977.

[18]Mei, C., and Rogers, J. L., Jr., "Application of NASTRAN to Large Deflection Supersonic Flutter of Panels," NASA TM-X 3478, Oct. 1976, pp. 67–97.

[19]Bhimaraddi, A., "Nonlinear Free Vibration Analysis of Composite Plates with Initial Imperfections and In-Plane Loading," *International Journal of Solids and Structures*, Vol. 25, No. 1, 1989, pp. 33–43.